Efficiency Analysis of BLDC Motor With Delta Connection According to Magnitude of Circulating Current

Ho-Young Lee[1,2], Kyoung-Soo Cha[1], Soon-O Kwon[1], Seung-Young Yoon[3], Chang-Hoon Seok[3], and Myung-Seop Lim[2]

[1]Advanced Mobility System Group, Korea Institute of Industrial Technology, Daegu 42994, Republic of Korea
[2]Department of Automotive Engineering, Hanyang University, Seoul 04763, Republic of Korea
[3]School of Electronic and Electrical Engineering, Kyungpook National University, Daegu 42994, Republic of Korea

In a delta connection, most of the battery voltage is applied directly to the motor's phase terminals, resulting in a voltage that is root three times higher than in a wye connection. This characteristic makes delta connections suitable for low-voltage, high-speed systems. However, the presence of 3 n-th harmonic components in the phase back electromotive force (BEMF) of delta-connected motors can induce circulating currents that flow exclusively within the circuit. These circulating currents lead to additional Joule losses and degrade motor performance. This article analyzes the effect of circulating currents on motor efficiency according to different speeds and torques. The presented study models maintain a similar magnitude of the fundamental component of BEMF but differ in the magnitude of the third harmonic component. A six-step circuit was established to compare the currents, losses, and efficiencies of the study models using finite element analysis (FEA). The copper losses were categorized into those caused by the fundamental component of phase current and those caused by the circulating currents. Subsequently, the efficiencies of the study models were compared across different speed and torque ranges, accounting for the separated copper loss components and iron losses. The results show that the improved model achieves an efficiency that is more than 18% higher than that of the basic model in the low-speed and low-torque areas. Finally, the study models were manufactured and evaluated through testing.

***Index Terms*— Brushless dc motor, circulating current, copper loss, delta winding, efficiency, harmonic phase current, six-step circuit, surface mounted permanent magnet synchronous motor.**

I. Introduction

THE brushless direct current motor (BLDC) enhances reliability and durability by eliminating the brushes and commutators typically found in conventional direct current motors. This design results in high efficiency and power density, making BLDC motors widely applicable across various industries due to their straightforward driving methods.

The BLDC motors can be classified into two types based on their stator winding configurations: wye and delta connections. In a delta connection, each coil's end is continuously connected to the start of another coil, as illustrated in Fig. 1. In this configuration, most of the battery voltage except for the voltage drop caused by the controller's switching elements is applied directly to the motor's phase terminals. Consequently, the voltage in a delta connection is root three times higher than that in a wye connection. This characteristic makes delta connections particularly suitable for applications like drones and power tools that require high-speed operation at low voltages.

However, delta connections can lead to circulating currents when the phase back electromotive force (BEMF) contains 3 n-th harmonic components, where n is an odd integer such as 1, 3, and 5 [1]. These circulating currents contribute to additional Joule losses, distort torque, and negatively affect vibration and noise levels. They may also result in magnetic saturation of the core and irreversible demagnetization of the permanent magnets [2]. Importantly, these currents cannot be directly measured at the motor's three lead wires.

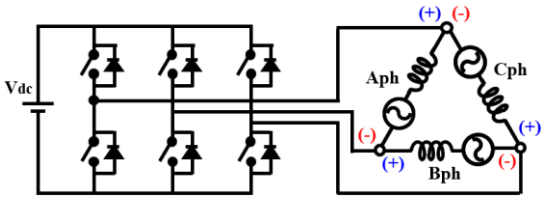

Fig. 1. Delta connected six-step circuit.

Recent research has actively explored the phenomenon of circulating currents. For example, in [3], circulating currents were defined as functions of electrical parameters such as BEMF, resistance, and inductance using voltage equations in the *abc* frame. Study [4] analyzed how design factors including slot opening width, height, yoke thickness, and pole angle of surface-mounted permanent magnet synchronous motors (SPMSM) affect circulating currents through FEA. However, there is a scarcity of studies that separate losses by speed and torque while quantitatively comparing motor efficiency. Moreover, few studies have measured and compared motor efficiency while considering circulating currents in prototypes with identical BEMF conditions. This article investigates the effect of circulating currents on motor efficiency across varying speeds and torques. Copper losses are categorized into those caused by the fundamental component of phase current and those resulting from circulating currents. Ultimately, this study compares efficiency based on different speed and

Received 14 June 2024; revised 28 August 2024; accepted 14 September 2024. Date of publication 23 September 2024; date of current version 26 November 2024. Corresponding author: M.-S. Lim (e-mail: myungseop@hanyang.ac.kr).

Color versions of one or more figures in this article are available at https://doi.org/10.1109/TMAG.2024.3465879.

Digital Object Identifier 10.1109/TMAG.2024.3465879

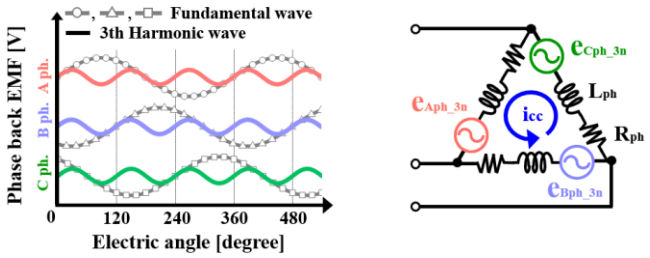

Fig. 2. Circulating current caused by the third harmonic component of phase BEMF. (a) Waveform of third harmonic component and (b) delta connection.

torque ranges, accounting for separated copper losses and iron losses.

II. Analytical Expression

Under balanced conditions, the vector sum of the three-phase sinusoidal voltages in a PMSM is zero. However, in a series-connected delta connection, if the harmonics components are included in the phase voltage, the in-phase 3 n-th harmonics voltage components add up to each other as shown in Fig. 2(a). Hence, these harmonics voltage components generate the circulating currents dependent on the resistance and inductance of the motor as shown in Fig. 2(b).

The circulating current can be expressed as follows [3]:

$$i_{cc} = \sum_{\substack{\nu=3k \\ k=1,3,5,\ldots}} \frac{\nu\omega_s\lambda_{\mathrm{PM},\nu}}{\sqrt{(\nu\omega_s(L_a+2M_{ab}))^2+R_s^2}} \sin(\nu\theta-\theta_\nu) \quad (1)$$

where the amplitude of the circulating current is

$$I_{cc} = \frac{\nu\omega_s\lambda_{\mathrm{PM},\nu}}{\sqrt{(\nu\omega_s(L_a+2M_{ab}))^2+R_s^2}} \quad (2)$$

where θ is the rotor electrical position, θ_ν is the angle between $\lambda_{\mathrm{PM},1}$ and $\lambda_{\mathrm{PM},\nu}$. Also, ω_s is the rotor's electrical speed and $\lambda_{\mathrm{PM},\nu}$ is the νth harmonics components of PM phase flux linkage. L_a and M_{ab} are the self and mutual inductances of phase respectively and R_s is the winding resistance.

The amplitude of the circulating current is limited by the electrical parameters including the stator resistance, inductances, and 3 n-th harmonics components of PM flux linkage. Also, as the speed increases, the reactance in (2) becomes much larger than the winding resistance. Therefore, the amplitude of the circulating current converges to a specific value.

III. Performance Comparison Using FEA

This chapter presents the basic and improved models with different phase BEMF waveforms. As illustrated in Fig. 3(a), the basic model features square-shaped permanent magnets, whereas the improved model, shown in Fig. 3(b), has rounded magnet surfaces. According to (2), circulating currents are generated by the 3 n-th harmonic components of the phase BEMF. To reduce these harmonic components, the improved model modifies the angle and edge thickness of the permanent magnets, as depicted in Fig. 3(c). The center thickness of the permanent magnets remains the same as in the basic model, ensuring that the mechanical air-gap length is consistent across both models. As a result, as shown in Fig. 4(a), the phase BEMF waveform of the improved model is closer to a sine wave compared to that of the basic model. Additionally, Fig. 4(b) illustrates that the basic model exhibits a high magnitude of the third harmonic component, while the improved model has almost none. Importantly, the magnitudes of the fundamental component of the phase BEMF are nearly identical in both models. The specifications of these models are summarized in Table I.

TABLE I
Specification of Study Models

Item	Unit	Value	
		Basic model	Improved model
Number of poles and slots	-	12/36	12/36
Pole angle	deg.	25.0	24.0
Edge thickness of PM	mm	2.5	1.5
1st component of Ph. BEMF (1,000rpm)	V	6.37	6.36
3rd component of Ph. BEMF (1,000rpm)	V	1.15	0.17

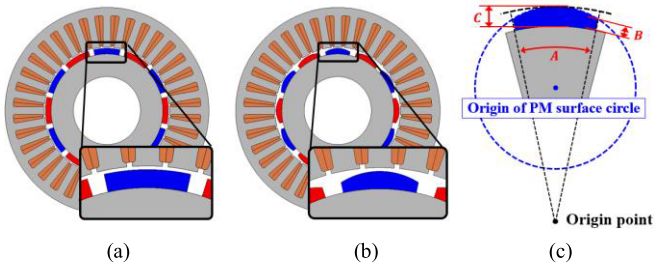

Fig. 3. Study models. (a) Basic model. (b) Improved model. (c) Design factor of permanent magnet.

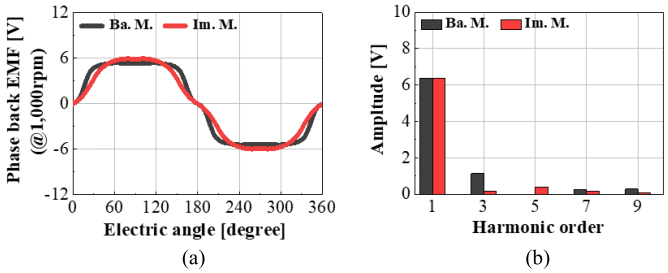

Fig. 4. Phase BEMF. (a) Waveform. (b) Harmonic analysis.

A. Circulating Current at No-Load Condition

As shown in Fig. 2(b), the circulating currents of the two models were analyzed using a delta connection circuit in an open-circuit configuration. At 4000 r/min, Fig. 5(a) demonstrates that the circulating current in the basic model is significantly higher than that in the improved model. Additionally, Fig. 5(b) indicates that the analytical results for the circulating current amplitude derived from (2) closely match the FEA results, with an error of less than 5%. The self and mutual inductances were estimated based on FEA by applying an arbitrary current to one phase and utilizing the flux

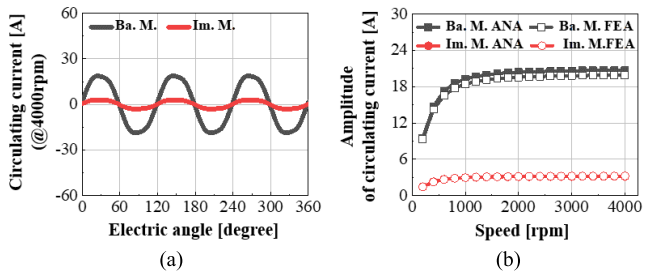

Fig. 5. Circulating current. (a) Waveform at 4000 r/min. (b) Amplitude of circulating current according to speed.

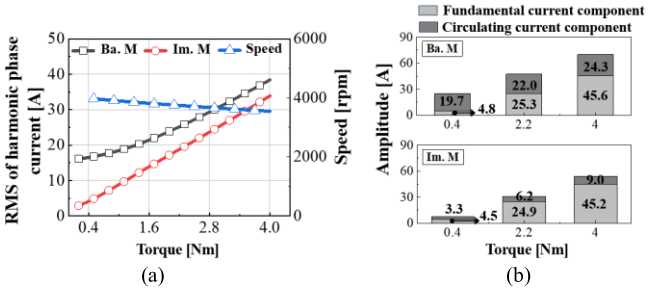

Fig. 6. Harmonic phase current. (a) RMS of harmonic phase current due to load. (b) Amplitude of fundamental and circulating current components.

linkage. As the speed increases, both the analytical and FEA results for the amplitude of the circulating current converge to a specific value.

B. Harmonic Phase Current

The study model was configured with a six-step circuit, as shown in Fig. 1, to analyze the harmonic phase currents at 24 V based on the load. The phase current was applied in phase with the motor's phase BEMF.

As illustrated in Fig. 6(a), the rms of the harmonic phase current in the improved model tends to increase proportionally with torque. In contrast, the basic model exhibits a certain magnitude of harmonic phase current in the low torque region due to circulating current. Fig. 6(b) separates the harmonic phase current into fundamental and circulating current components. At 0.4 Nm, the circulating current in the basic model is four times higher than the fundamental component. Also, as torque increases, the circulating current tends to increase slightly as well. This is due to the saturation of the core's flux density, which generates 3 n-th harmonic components in the phase voltage as the current rises with the increasing torque. However, at 4.0 Nm, the fundamental component, which increases with torque, is significantly higher than the circulating current. Consequently, the fundamental component and circulating current exhibit different tendencies depending on the torque.

C. Losses and Efficiency

As shown in Fig. 7, the copper losses were separated into losses caused by the fundamental phase current and losses caused by the circulating current. The mechanical losses were ignored. The eddy current losses in the permanent magnet

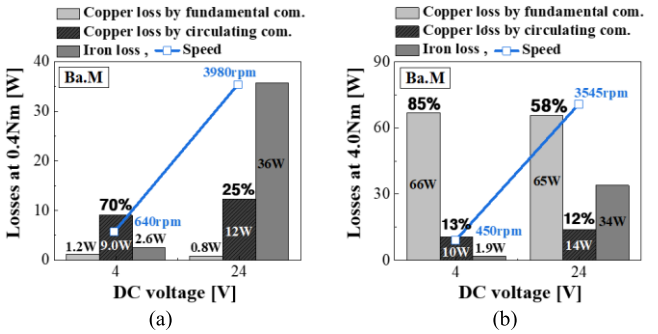

Fig. 7. Loss distribution at dc voltages of 4 and 24 V. (a) 0.4 Nm. (b) 4.0 Nm.

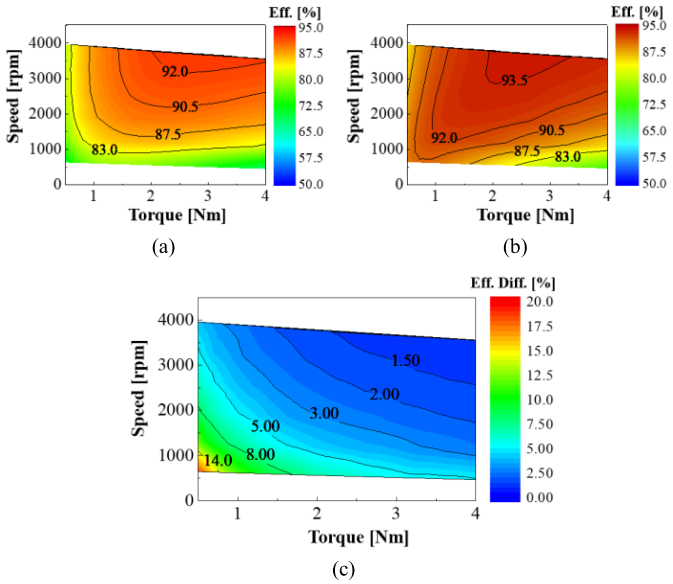

Fig. 8. Efficiency map. (a) Basic model. (b) Improved model. (c) Efficiency difference between improved model and basic model.

were very small compared to other losses, so they were omitted from Fig. 7. However, these eddy current losses in the permanent magnet were considered in the efficiency map in Fig. 8.

First, as illustrated in Fig. 7(a), for the basic model at 4 V, the copper loss due to circulating current is the largest, accounting for about 70% of the total losses. In contrast, at the higher speed of 24 V, the proportion of copper loss due to circulating current decreases to about 25% as iron losses increase.

Next, in Fig. 7(b), the copper loss associated with the fundamental current is the highest, making up approximately 85% at 4 V and about 58% at 24 V. Consequently, the copper loss due to circulating current falls to around 13% at 4 V and 12% at 24 V, significantly lower than the proportion seen in Fig. 7(a). These results suggest that the efficiency reduction caused by the circulating current is most pronounced in the low-torque, low-speed range, while its impact is minimal in the high-torque, high-speed range.

Finally, based on the losses derived from the FEA results, the efficiency of the study models was compared, as shown in Fig. 8. In Fig. 8(c), the efficiency difference between the study models gradually increases as the low-torque and low-

(a) (b) (c)

Fig. 9. Dynamo load system and BEMF testing of prototype. (a) Rotor core and PM of the prototype. (b) Test setup. (c) Waveform and harmonic analysis.

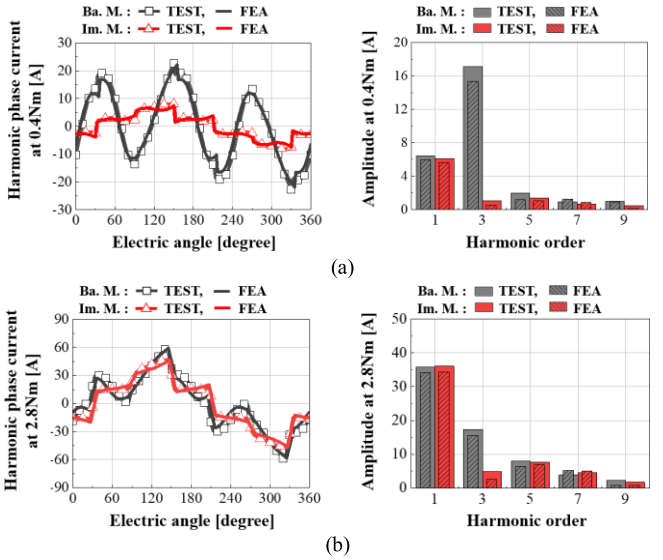

(a) (b)

Fig. 10. Harmonic phase current waveforms and harmonic analysis from TEST and FEA. (a) Torque 0.4 Nm. (b) Torque 2.8 Nm.

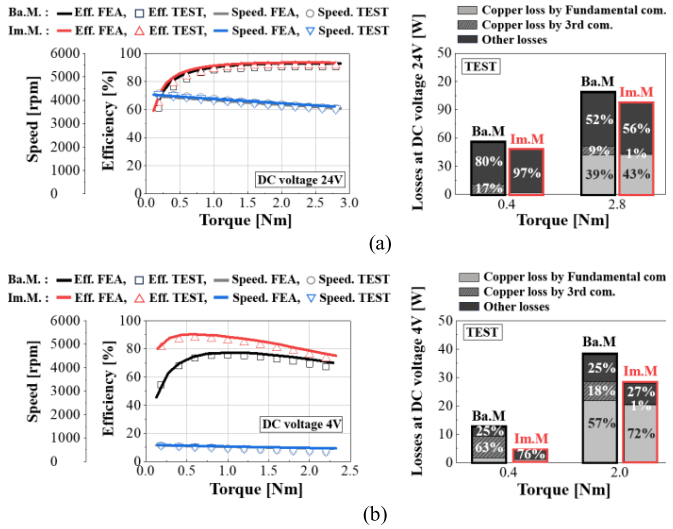

(a) (b)

Fig. 11. Efficiency, speed, and losses from TEST and FEA. (a) DC voltage 24 V. (b) DC voltage 4 V.

speed area is approached. At 0.5 Nm and 640 r/min, the efficiency difference is substantial, around 18%. For even lower torque and speed areas, this difference will be greater. Conversely, in the high-speed, high-torque area, the efficiency difference between the study models is minimal. At 4.0 Nm and 3550 r/min, the difference is only about 1.0%. In the low-speed, high-torque areas and the high-speed, low-torque areas, the efficiency difference ranges from 3.0% to 5.0%, which is not insignificant.

IV. Experimental Result

As shown in Fig. 9(a), the cores and permanent magnets of the study models were manufactured. To prevent the permanent magnets from detaching from the rotor core due to centrifugal force at high speeds, protrusions were added to the surface of the rotor core. In Fig. 9(b), each phase terminal was connected outside the housing to measure the phase current of the motor. The test equipment was utilized to measure the speed, torque, current, and voltage of the motor. As indicated in Fig. 9(c), the FEA results and the test results for the phase BEMF waveform are in good agreement. The FEA model of the prototype includes the protrusions on the rotor core surface.

Next, the harmonic phase current waveforms of the prototype were measured at 0.4 and 2.8 Nm. The controller used a six-step driver, applying square wave current in phase with the motor's phase back EMF. As shown in Fig. 10(a), the current waveforms of the study models exhibit significant differences. The harmonic analysis reveals that, in the case of the basic model, the third harmonic component of the phase current is approximately three times larger than the fundamental component. The difference in the third harmonic component between the basic and improved models is attributed to the effects of circulating currents. However, at 2.8 Nm, as shown in Fig. 10(b), the phase current waveforms of the study models become similar. The harmonic analysis indicates that the fundamental component of the phase current is about twice as large as the third harmonic component, meaning the distortion of the phase current waveform due to circulating currents is relatively less in the high-torque area compared to the low-torque area.

Finally, the efficiency, speed, and losses of the prototypes were compared at applied voltages of 24 and 4 V. As shown in Fig. 11(a), at 24 V, the study models demonstrated similar efficiency trends, with an efficiency difference of about 3% at 0.4 Nm. The proportion of copper losses due to circulating currents is only 17% because other losses are relatively high at this torque. At 4 V, as shown in Fig. 11(b), the efficiency difference between the study models is significant in the low-torque area, reaching about 18% at 0.4 Nm. Here, the proportion of copper losses due to circulating currents is quite high, approximately 63%. In the high-torque range, however, the copper losses attributed to the fundamental component of

the phase current are high, resulting in a lower proportion of copper losses due to circulating currents.

V. Conclusion

This article analyzes the effect of circulating currents on the efficiency of delta-connected BLDC motors at various speeds and torques. The circulating currents tend to maintain a certain magnitude unless the speed is very low. When the core flux density becomes saturated, the magnitude of circulating currents can be influenced by changes in the third harmonic component of the phase voltage. In low-speed, low-torque areas where other loss components are low, the circulating currents have a critical negative effect on motor efficiency. For the studied models, the efficiency difference was as much as 18%. In contrast, in high-speed and high-torque areas, the efficiency difference was less than 1.5%, showing minimal effect.

Acknowledgment

This work was supported by the Technology Innovation Program (No. 00250833) funded By the Ministry of Trade, Industry & Energy (MOTIE, Korea).

References

[1] S. M. Raziee, O. Misir, and B. Ponick, "Winding function approach for winding analysis," *IEEE Trans. Magn.*, vol. 53, no. 10, pp. 1–9, Oct. 2017.

[2] F. J. T. E. Ferreira, A. M. Silva, S. M. A. Cruz, and A. T. De Almeida, "Comparison of losses in star- and delta-connected induction motors with saturated core," in *Proc. IEEE Int. Electr. Mach. Drives Conf. (IEMDC)*, May 2017, pp. 1–8.

[3] S. Mukundan, H. Dhulipati, Z. Li, M. S. Toulabi, J. Tjong, and N. C. Kar, "Coupled magnetic circuit-based design of an IPMSM for reduction of circulating currents in asymmetrical star–delta windings," *IEEE Trans. Transport. Electrific.*, vol. 8, no. 2, pp. 2971–2984, Jun. 2022.

[4] L. Zhu, S. Niu, Y. C. Wang, and C. Wang, "Advanced design and operation consideration for close-connected winding permanent-magnet brushless DC machine," *IEEE Trans. Appl. Supercond.*, vol. 26, no. 4, pp. 1–4, Jun. 2016.